Doc Ophthalmol
DOI 10.1007/s10633-010-9227-0

ORIGINAL RESEARCH ARTICLE

Functional involvement of cone photoreceptors in advanced glaucoma: a multifocal electroretinogram study

Ajoy Vincent · Rohit Shetty · Sathi A. V. Devi · Mathew K. Kurian · Ramgopal Balu · Bhujang Shetty

Received: 23 May 2009 / Accepted: 8 March 2010

Abstract The purpose of the study is (1) to demonstrate the anatomical variation of cone photoreceptor density across normal retina as a sectoral amplitude asymmetry of photopic multifocal electroretinogram (mfERG) and (2) to study the potential presence of sequential or differential, functional cone photoreceptor damage in glaucoma using this amplitude asymmetry. A 37-Block scaled mfERG was recorded from 22 controls and 27 glaucoma subjects. The N1 and P1 amplitudes of averaged responses from corresponding zones nasal and temporal to fovea were analyzed for asymmetry in controls and glaucoma subjects. Amplitude asymmetry was demonstrable for both N1 ($p < 0.001$) and P1 ($p < 0.001$) parameters in control subjects. Although this amplitude asymmetry was preserved in glaucoma subjects with moderate field defects, it was not demonstrable in patients with advanced field defects. The anatomical variation in cone photoreceptor distribution across normal retina is demonstrated as an amplitude asymmetry in first order kernel responses of mfERG. The cone photoreceptors in the region nasal to fovea appear to be affected only in advanced glaucoma possibly suggesting that photoreceptors could follow a sequential damage like the overlying neuroretinal rim in glaucoma.

Keywords Electroretinography · Glaucoma · Retinal cone photoreceptor cells · Retinal bipolar cells · Optical coherence tomography

A. Vincent (✉) · R. Shetty · B. Shetty
Department of Electrophysiology, Narayana Nethralaya, Super Specialty Eye Hospital and Post Graduate Institute of Ophthalmology, 121/C, Chord Road, Rajaji Nagar 1st 'R' Block, Bangalore 560010, India
e-mail: ajoytvincent@rediffmail.com

S. A. V. Devi · R. Balu
Department of Glaucoma, Narayana Nethralaya, Super Specialty Eye Hospital and Post Graduate Institute of Ophthalmology, 121/C, Chord Road, Rajaji Nagar 1st 'R' Block, Bangalore 560010, India

M. K. Kurian
Department of Epidemiology and Medical Statistics, Narayana Nethralaya, Super Specialty Eye Hospital and Post Graduate Institute of Ophthalmology, 121/C, Chord Road, Rajaji Nagar 1st 'R' Block, Bangalore 560010, India

Introduction

The multifocal electroretinogram (mfERG) technique records multiple local responses from the central retina [1, 2]. The current knowledge suggests that the 'N1' wave of first order kernel response of photopic mfERG has its origin from the cone photoreceptors and cone 'OFF' bipolar cells; whereas the 'P1' wave arises from the cone 'ON' and cone 'OFF' bipolar cells [3, 4]. The density of human cone photoreceptors has been reported to be high, in the quadrant nasal to fovea, than the quadrant temporal to fovea at all eccentricities [5, 6]. We hypothesized that the anatomical difference in cone photoreceptor density

Published online: 25 March 2010

across the retina could be demonstrated as an amplitude asymmetry of the N1 wave across the fovea in healthy controls.

In glaucoma, the neuroretinal rim (NRR) thins in a sequential manner [7–13]; nasal NRR and papillomacular bundle being the last to be affected. A sequential or differential functional impairment of outer retinal layers underlying the ganglion cell layer could occur in the natural history of progression of glaucoma. Previous histological studies conducted on enucleated glaucomatous eyes, demonstrated varied results with regard to photoreceptor layer involvement [14, 15]. An attempt therefore has been made to assess if the amplitude asymmetry in mfERG could be used to detect the potential presence of sequential or differential, functional cone photoreceptor damage in the central ±24° in glaucoma.

Methods

This is a prospective, cross-sectional, case–control study. The protocol adhered to the Declaration of Helsinki and was approved by Institutional Ethical Board. All the subjects signed informed consent after the procedures were well explained to them.

Human subjects

The mfERG was recorded from 22 eyes of 22 control subjects (group A; range: 27–74 years, median age–54 years) and 27 eyes of 27 glaucoma subjects (Range 27–79 years). All glaucoma subjects had undergone Humphreys field analysis and they either had moderate (group B; $N = 13$) or advanced (group C; $N = 14$) visual field defects as defined in Hodapp, Parrish and Anderson's classification [16]. The median age of glaucoma patients in group B was 58 (range 27–78 years); the median in group C was 55 (range 38–79 years). Seventeen patients had primary open angle glaucoma (POAG), and ten had primary angle closure glaucoma (PACG). All glaucoma patients underwent detailed ophthalmological evaluation including best corrected distant and near vision assessment, applanation tonometry, gonioscopy, slit lamp biomicroscopic evaluation of optic disc, Humphreys 30—2 visual field analysis and retinal nerve fiber layer (RNFL) thickness measurement by stratus optical coherence tomography (OCT). All subjects of POAG or PACG with a best corrected distance visual acuity >20/40 and best corrected near visual acuity of N6 were included. Any subject with co-existing retinal or optic nerve pathology was excluded. Patients on miotics and cases of secondary glaucoma were excluded. Subjects with systemic diseases like diabetes mellitus and hypertension were also excluded. The intraocular pressure (IOP) of all the subjects was on adequate control (<21 mm Hg) at which sitting mfERG was done.

Before recording mfERG, the pupil was fully dilated with 1% tropicamide and 2.5% phenylepherine. The cornea was anaesthetized with 0.5% proparacaine hydrochloride, and jet electrodes were used for recording. All subjects were given full refractive correction at the testing distance of 30 cm.

Stimulation

The mfERG was recorded using the Metrovision ERG system (Pérenchies, France). The stimulus array

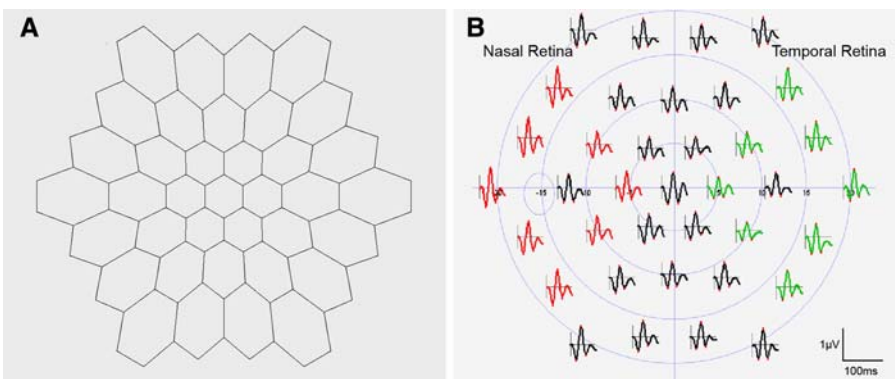

Fig. 1 **a** The 37 Block scaled hexagonal stimulus array; **b** demonstrate the corresponding zones nasal and temporal to fovea used in the analysis

consisted of 37 scaled hexagons (Fig. 1a; central hexagon 4°, peripheral hexagon 8°) covering ±24° of the visual field. Relatively low number of hexagons was used to obtain high-intensity response from each hexagon. The stimulus array was displayed on a high-resolution cathode ray tube monitor of a mean luminance of 200 cd/m^2 and a contrast of 95%. A uniformly illuminated background of 30 cd/m^2 surrounded the stimulus screen. Each element of the sequence constituted of 3 bright frames followed by 4 dark frames achieving a stimulus frequency of 17.14 Hz (120 Hz/7). This was done for reducing temporal interactions between responses to successive stimuli. The low- and high-pass filters were kept at 72 and 0.1 Hz, respectively. The amplification gain was 20,000, and the sampling rate was 1 kHz. An experimental run consisted of a sequence length of 511, which was repeated twenty times so as to achieve a very high signal to noise ratio. The total recording time was 9 min 30 s. The first order kernel responses from each of the 37 scaled stimulus patches were converted into response densities and responses from selected regions were analyzed.

Methods of analysis

The responses were averaged from selected hexagons nasal to fovea and corresponding hexagons temporal to fovea (Fig. 1b); converted to ratios (average of response densities nasal to fovea: average of response densities temporal to fovea) and analyzed. These hexagons were chosen because: (a) the cone photoreceptor density is highest along the horizontal raphe nasal to the fovea and (b) this region includes papillomacular bundle and nasal RNFL both of which are affected late in glaucoma. The response from the zone adjacent and overlying the optic nerve head and the corresponding zone temporal to fovea were not considered as photoreceptor density in and around the optic nerve head is less.

Statistical analysis

Paired '*t*' test was done in control subjects (group A) to evaluate asymmetry between averaged responses nasal and temporal to fovea for both amplitude and implicit time parameters of N1 and P1. Amplitude asymmetry ratios were then calculated for all the three groups; group A (control), group B (glaucoma subjects with moderate field defects) and group C (glaucoma subjects with severe field defects). One-way ANOVA and post hoc Bonferroni tests were done to measure the difference among the three groups with regard to age, N1 amplitude asymmetry and P1 amplitude asymmetry. Further, unpaired '*t*' test was done to test for any difference in N1 and P1 waveform parameters between subjects with POAG and PACG.

Results

Age characteristics in the three groups

The mean age in groups A, B and C were 50.23 ± 14.79, 57.38 ± 15.38 and 56.43 ± 10.60, respectively. One-way ANOVA analysis did not show any statistically significant difference in age between the groups ($p = 0.255$).

Analysis of control subjects

The mean of averaged N1 and P1 waveform parameters from zones nasal and temporal to fovea in group A are given in Table 1. Paired '*t*' test showed statistically significant difference between the zones for both N1 and P1 amplitude parameters ($p < 0.001$ for both) but not for N1 and P1 implicit time parameters ($p = 0.69$ and $p = 0.09$, respectively). The amplitude asymmetry was calculated as a ratio (average of response densities nasal to fovea: average of response densities temporal to fovea) for both N1 and P1 parameters, and the mean for group A was found to be 1.24 and 1.19, respectively.

Table 1 Mean amplitude and implicit time parameters for N1 and P1 in the zone nasal and temporal to fovea in controls

$N = 22$	Mean ± SD	
	Nasal zone	Temporal zone
N1 amplitude (nV/deg^2)	−26.641 ± 6.043	−21.505 ± 4.949
P1 amplitude (nV/deg^2)	53.432 ± 11.347	45.068 ± 10.442
N1 implicit time (ms)	23.727 ± 1.334	23.79 ± 1.41
P1 implicit time (ms)	42.364 ± 1.544	42.239 ± 1.731

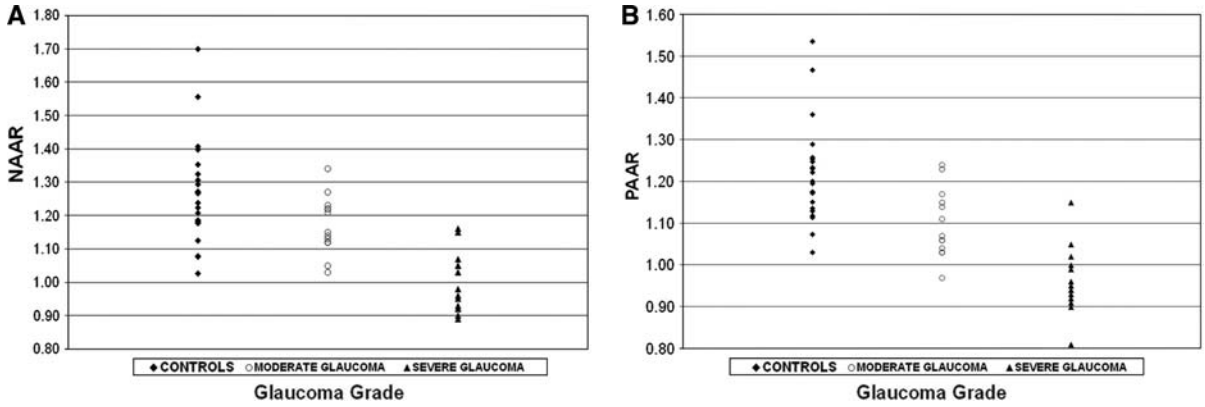

Fig. 2 Scatter plot showing amplitude asymmetry ratio between zones nasal and temporal to fovea for both N1 and P1 amplitudes in each subject of the three groups. *X*-axis represents the group and *Y*-axis represents amplitude asymmetry ratio. Note that N1 and P1 amplitude asymmetry ratios are <1 in few cases of advanced glaucoma. **a** Scatter plot shows amplitude asymmetry ratio for N1 amplitude in all the three groups. **b** Scatter plot shows amplitude asymmetry ratio for P1 amplitude in all the three groups

Comparison of amplitude asymmetry ratio among control subjects, glaucoma subjects with moderate field defects and glaucoma subjects with advanced field defects

The N1 amplitude asymmetry ratio (NAAR) and P1 amplitude asymmetry ratio (PAAR) for each subject in the three groups are shown in Fig. 2a and b, respectively. The mean NAAR in the groups A, B and C are 1.24, 1.17 and 1.00, respectively (Table 2). The mean PAAR in groups *A*, *B* and *C* are 1.19, 1.10 and 0.95, respectively (Table 2).

One-way ANOVA analysis showed statistically significant difference among the three groups for both NAAR ($p < 0.001$) and PAAR ($p < 0.001$). Post hoc test showed a statistically significant difference between groups A and C for both NAAR ($p < 0.001$) and PAAR ($p < 0.001$). Post hoc test also showed a statistically significant difference between groups B and C [NAAR ($p < 0.001$); PAAR ($p < 0.001$)] but not between groups A and B [NAAR ($p = 0.167$); PAAR ($p = 0.06$). Figure 3 shows averaged mfERG responses from the corresponding zones nasal and temporal to fovea of 2 subjects from each group.

Unpaired '*t*' test did not reveal statistically significant difference for NAAR ($p = 0.17$), and PAAR ($p = 0.27$) between subjects with POAG ($N = 17$) and PACG ($N = 10$). There was no statistically significant difference in N1 ($p = 0.33$) and P1 ($p = 0.75$) implicit time parameters between subjects with POAG and PACG.

Analysis of individual subjects in advanced visual field defect group

The group C subjects, with NAAR and PAAR values ≥ 1.08 and ≥ 1.02, respectively, were further assessed. These cutoff values for asymmetry were obtained from group B subjects by calculating their mean minus standard deviation for the respective parameter. Three patients (P3, P14 and P18) had values greater than the cutoff for both NAAR and PAAR, thus demonstrating amplitude asymmetry. These three patients had a mean RNFL thickness of 50.8 μm when compared to the other eleven in group C (mean RNFL thickness—42.9 μm).

Table 2 Mean amplitude asymmetry ratio for N1 and P1 amplitude in the groups

Amplitude asymmetry parameter	Group	Mean ± Std. deviation
N1 Amplitude	Normal	1.24 ± 0.12
	Moderate visual field defect	1.17 ± 0.09
	Advanced visual field defect	1.00 ± 0.08
P1 Amplitude	Normal	1.19 ± 0.10
	Moderate visual field defect	1.10 ± 0.08
	Advanced visual field defect	0.95 ± 0.09

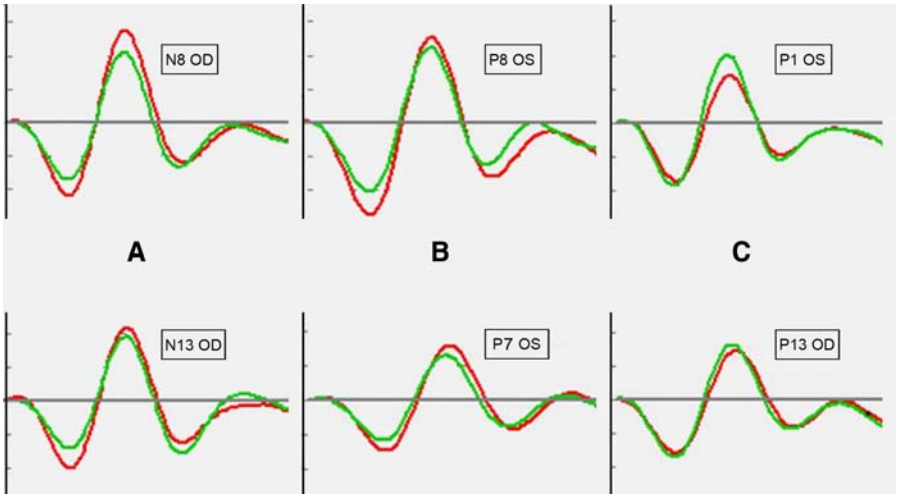

Fig. 3 Averaged mfERG recordings from two subjects in each group. *Red* tracing represent averaged mfERG from the quadrant nasal to the fovea, whereas *green* tracing represent averaged responses from the quadrant temporal to fovea. The *x*-axis represents time (100 ms total) and in the *y*-axis each division represents 500 nanovolts. **a** Shows recordings from two group A subjects. The N1 and P1 amplitude parameter from the zone nasal to fovea is larger than that obtained from the corresponding zone temporal to fovea. **b** Averaged responses from two group B subjects showing characteristics similar to group A subjects. **c** Averaged mfERG recordings from two group C subjects demonstrating the fact that the response from the zone nasal to fovea is equal or smaller than the response from the corresponding zone temporal to fovea

Discussion

In this study, both N1 and P1 averaged response amplitudes are significantly higher in the quadrant nasal to fovea than those obtained from the corresponding zone temporal to fovea in controls (group A). Previous anatomical studies have demonstrated a significantly high cone photoreceptor density in the region nasal to fovea in enucleated human and monkey eyes [5, 6, 17, 18]. This naso-temporal cone density difference ratio is reported to be 1.25 at the optic disc (along horizontal meridian), further increasing to 1.40–1.45 at 9 mm eccentricity from the fovea [6]. The mean value of NAAR in group A is 1.24 ± 0.12. Since the cone photoreceptors contribute to the N1 waveform of mfERG, this amplitude asymmetry between corresponding quadrants nasal and temporal to fovea in group A represents the reported histological asymmetry. The visual field covered in the study being $\pm 24°$, a NAAR value of 1.24 correlates well with the reported histological naso-temporal cone density difference within that eccentricity. Previous studies have described a latency component of naso-temporal disparity in mfERG across the retina in monkeys [19, 20] and humans [20, 21]. At higher contrast, since outer retinal contributions are predominant [22], only a small latency difference could be demonstrated [21]. In this study, the authors have used high contrast and high luminosity to extract activity from the cone photoreceptors and bipolar cells. There is no implicit time difference demonstrated across the retina for both N1 and P1 parameters in group A subjects. Further, the authors introduced 4 dark frames between light presentations to reduce temporal interaction. Higher order kernel responses were not detectable in group A subjects confirming the reduced temporal interactions; implying that ganglion cell contribution to the first order responses in this study can be presumed to be negligible.

The NRR of the optic nerve head is broadest in the inferior region, followed by superior, nasal and temporal regions [23, 24]. In glaucoma, a primary ganglion cell disease [25], the NRR thins in a sequential manner [7–13]; nasal NRR and papillomacular bundle being the last to be affected. Hence, a sequential or differential involvement of cone photoreceptors underlying the ganglion cell layer could occur in glaucoma and this has not been studied previously. Previous histological studies conducted on glaucomatous eyes report variably; some suggestive of photoreceptor preservation [14] whereas

others suggestive of photoreceptor loss [15]. Electrophysiological studies done with full field/flash ERG in glaucoma has shown changes in scotopic and/or photopic responses [26–28] suggesting generalized photoreceptor damage. The changes in ERG were found to be more pronounced in advanced cases [29–31]. However, a more recent study in experimental glaucoma reported normal photopic amplitude parameters [32]. The cause for photoreceptor impairment in glaucoma has been attributed to multiple factors, including retrograde cell degeneration [26–29]. In this study, the N1 amplitude asymmetry demonstrated in control subjects was also seen in glaucoma subjects with moderate visual field defects. The explanation for this amplitude asymmetry preservation in group B subjects being; the papillomacular bundle is known to be preserved in moderate glaucoma and the underlying cone photoreceptors do not develop retrograde degeneration at this stage. However, both N1 and P1 amplitude asymmetry were not demonstrable in glaucoma subjects with advanced visual field defects. The absence of N1 amplitude asymmetry in group C patients suggest significant cone photoreceptor impairment nasal to fovea in advanced glaucoma. The papillomacular bundle and nasal NRR are known to be affected in advanced glaucoma. This could lead to retrograde degeneration of higher number of underlying cone photoreceptors causing disappearance of N1 amplitude asymmetry in advanced cases. The reversal of NAAR and PAAR was seen in eight group C subjects (P1, P2, P13, P15, P16, P17, P19 and P10). The reversal of NAAR further confirms this differential cone photoreceptor impairment in advanced glaucoma. However, this functional cone photoreceptor impairment need not necessarily translate into a structural one, which possibly explains the presence of normal cone density in glaucoma as reported earlier [14].

Further analysis revealed three group C subjects (P3, P14 and P18) to have preserved amplitude asymmetry. The mean RNFL was thicker in this subset of patients when compared to others in this group. The relatively thicker RNFL could have contributed to less severe retrograde degeneration of underlying photoreceptors in these three subjects.

In conclusion, the N1 amplitude asymmetry demonstrated in first order kernel responses of photopic mfERG in control subjects is the functional equivalent of the reported histological asymmetry of cone photoreceptors across the retina. The cone photoreceptors in the region nasal to fovea appear to be affected only in advanced glaucoma possibly suggesting that photoreceptors could follow a sequential damage like the overlying NRR. The presence of P1 amplitude asymmetry in control subjects could suggest a regional asymmetry of bipolar cells distribution across the retina. Previous mfERG and multifocal pattern ERG (mfPERG) studies reported limited success in localizing inner retinal layer damage in glaucoma [20, 33–35]. In this study, the authors have demonstrated noticeable regional outer retinal dysfunction in the central $\pm 24^{\circ}$ in advanced glaucoma.

Acknowledgments The authors are thankful to Dr. Rashmi Rodriguez and Dr. Pretesh R Kiran (St. John's medical college, Bangalore) for assistance in statistics. The authors are thankful to Dr. Charlier, J (Metrovision, France) for customizing mfERG stimulus. The authors are thankful to Dr. Somashekhar N and Dr. Prasanth CN (Narayana Nethralaya, Bangalore) for assistance in recruiting control subjects. The authors are thankful to Mrs. Vijayalakshmi Pires (PhD Eng Litt) and Mrs. Thaliath, NMAF for assistance in English language editing. The authors are thankful to Mrs Revathi MP for assistance in mfERG recording and Mr. Muhammed Naizal T (Narayana Ophthalmic Multimedia Art Department) for assistance in figures.

Conflict of interest statements No conflict for any author.

Financial disclosure None of the authors have any financial interests to disclose.

References

1. Sutter EE (1991) The fast m-transform: a fast computation of cross-correlations with binary m-sequences. Soc Ind Appl Math 20:686–694
2. Sutter EE, Tran D (1992) The field topography of ERG components in man, I: the photopic luminance response. Vis Res 32:433–466
3. Hood DC, Bach M, Brigell M, Keating D, Kondo M, Lyons JS, Palmowski-Wolfe AM (2008) ISCEV guidelines for clinical multifocal electroretinography (2007 edition). Doc Ophthalmol 116:1–11
4. Hood DC, Frishman LJ, Saszik S, Viswanathan S (2002) Retinal origins of the primate multifocal ERG: implications for the human response. Invest Ophthalmol Vis Sci 43(5):1673–1685
5. Jonas JB, Schneider U, Naumann GO (1992) Count and density of human retinal photoreceptors. Graefes Arch Clin Exp Ophthalmol 230(6):505–510
6. Curcio CA, Sloan KR, Kalina RE, Hendrickson AE (1990) Human photoreceptor topography. J Comp Neurol 292(4): 497–523

7. Hitchings RA, Wheeler CA (1980) The optic disk in glaucoma (IV. Optic disc evaluation in the ocular hypertensive patient). Br J Ophthalmol 64:232–239
8. Hitchings RA (1978) The optic disk in glaucoma (III. Diffuse optic disk pallor with raised intraocular pressure). Br J Ophthalmol 62:670–675
9. Hitchings RA, Spaeth GL (1977) The optic disk in glaucoma (II. Correlation of the appearance of the optic disc with the visual field). Br J Ophthalmol 61:107–113
10. Jonas JB, Fernández M, Stürmer J (1993) Pattern of glaucomatous neuroretinal rim loss. Ophthalmology 100: 63–67
11. Kirsch RE, Anderson DR (1973) Clinical recognition of glaucomatous cupping. Am J Ophthalmol 75:442–454
12. Pederson JE, Anderson DR (1980) The mode of progressive disc cupping in ocular hypertension and glaucoma. Arch Ophthalmol 98:490–495
13. Tuulonen A, Airaksinen PJ (1991) Initial glaucomatous optic disk and retinal nerve fiber layer abnormalities and the mode of their progression. Am J Ophthalmol 111:485–490
14. Kendell KR, Quigley HA, Kerrigan LA, Pease ME, Quigley EN (1995) Primary open angle glaucoma is not associated with photoreceptor loss. Invest Ophthalmol Vis Sci 36:200–205
15. Panda S, Jonas JB (1992) Decreased photoreceptor count in human eyes with secondary angle closure glaucoma. Invest Ophthalmol Vis Sci. 33:2532–2536
16. Hodapp E, Parrish RK, Anderson DR (1993) Clinical decisions in glaucoma. The CV: Mosby Co, St. Louis, pp 52–61
17. Wilker KC, Williams RW, Rakic P (1990) Photoreceptor mosaic: number and distribution of cones and rods in rhesus monkey retina. J Comp Neurol 297:499–508
18. Curcio CA, Millican CL, Allen KA, Kalina RE (1993) Aging of the human photoreceptor mosaic: evidence for selective vulnerability of rods in central retina. Invest Ophthalmol Vis Sci 34:3278–3296
19. Hood DC, Frishman LJ, Viswanathan S, Robson JG, Ahmed J (1999) Evidence for a substantial ganglion cell contribution to the primate electroretinogram (ERG): effect of TTX on the multifocal ERG in macaque. Vis Neurosci 16(3):411–416
20. Hood DC, Greenstein V, Frishman LJ, Holopigian K, Viswanathan S, Seiple W, Ahmed J, Robson JG (1999) Identifying inner retinal contributions to the human multifocal ERG. Vis Res 39:2285–2291
21. Sutter EE, Bears MA (1999) The optic nerve component of human ERG. Vis Res 39:419–436
22. Bearse MA, Sutter EE (1998) Contrast dependence of multifocal ERG components. Visual science and its application, OSA Technical Digest Series 24–27
23. Jonas JB, Gusek GC, Naumann GOH (1988) Optic disc, cup and neuroretinal rim size, configuration, and correlations in normal eyes. Invest Ophthalmol Vis Sci 29:1151–1158
24. DeLeón-Ortega JE, Arthur SN, McGwin G, Xie A, Monheit BE, Girkin CA (2006) Discrimination between glaucomatous and nonglaucomatous eyes using quantitative imaging devices and subjective optic nerve head assessment. Invest Ophthalmol Vis Sci 47:3374–3380
25. Quigley HA, Addicks EM, Green WR, Maumenee AE (1982) Optic nerve damage in human glaucoma. III. Quantitative correlation of nerve fiber loss and visual field defect in glaucoma, ischaemic optic neuropathy, papilledema and toxic neuropathy. Arch Ophthalmol 100:135–146
26. Karlberg B, Hedin A, Bjornberg K (1968) Electroretinography during short-term intraocular tension rise. Acta Ophthalmol 46:742–747
27. Alvis DL (1966) Electroretinographic changes in controlled chronic open angle glaucoma. Am J Ophthalmol 61:121–131
28. Bartl G, Benedikt O, Hiti H (1978) The effect of elevated intraocular pressure on the human ERG and VER. Graefes Arch Clin Exp Ophthalmol 207:275–279
29. Fazio DT, Heckenlively JR, Martin DA, Christensen RE (1986) The Electroretinogram in advanced open angle glaucoma. Doc Ophthalmol 63:45–54
30. Velton IM, Korth M, Horn FK (2001) The a-wave of the dark-adapted Electroretinogram in glaucomas: are photoreceptors affected? Br J Ophthalmol 85:397–402
31. Velton IM, Horn FK, Korth M, Velten K (2001) The b-wave of the dark-adapted Electroretinogram in patients with advanced asymmetrical glaucoma and normal subjects. Br J Ophthalmol 85:403–409
32. Viswanathan S, Frishman LJ, Robson JG, Harwerth RS, Smith EL (1999) The photopic negative response of the macaque electroretinogram: reduction by experimental glaucoma. Invest Ophthalmol Vis Sci 40:1124–1136
33. Hood DC, Greenstein VC, Holopigian K, Bauer R, Firoz B, Liebmann JM, Odel JG, Ritch R (2000) An attempt to detect glaucomatous damage to the inner retina with the multifocal ERG. Invest Ophthalmol Vis Sci 41:1570–1579
34. Hasegawa S, Takagi M, Usui T, Takada R, Abe H (2000) Waveform changes of the first order multifocal electroretinogram in patients with glaucoma. Invest Ophthalmol Vis Sci 41:1597–1603
35. Klistorner A, Graham SL, Martins A (2000) Multifocal pattern electroretinogram does not demonstrate localized field defects in glaucoma. Doc Ophthalmol 100:155–165